JOURNAL OF MATERIALS SCIENCE **37** (2002) 141 – 150

Effects of interface coating and nitride enhancing additive on properties of Hi-Nicalon SiC Fiber reinforced reaction-bonded silicon nitride composites

R. T. BHATT
U.S. Army Research Laboratory, Glenn Research Center, Cleveland, Ohio 44135, USA
E-mail: Ramakrishna.T.Bhatt@lerc.nasa.gov

D. R. HULL, J. I. ELDRIDGE
Glenn Research Center, Cleveland, Ohio 44135, USA

R. BABUDER
Case Western Reserve University, Cleveland, Ohio 44106, USA

Strong and tough Hi-Nicalon SiC fiber reinforced reaction-bonded silicon nitride matrix composites (SiC/RBSN) have been fabricated by the fiber lay-up approach. Commercially available uncoated and PBN, PBN/Si-rich PBN, and BN/SiC coated SiC Hi-Nicalon fiber tows were used as reinforcement. The composites contained ~24 vol% of aligned 14 μm diameter SiC fibers in a porous RBSN matrix. Both one- and two-dimensional composites were characterized. The effects of interface coating composition, and the nitridation enhancing additive, NiO, on the room temperature physical, tensile, and interfacial shear strength properties of SiC/RBSN matrix composites were evaluated. Results indicate that for all three coated fibers, the thickness of the coatings decreased from the outer periphery to the interior of the tows, and that from 10 to 30 percent of the fibers were not covered with the interface coating. In the uncoated regions, chemical reaction between the NiO additive and the SiC fiber occurs causing degradation of tensile properties of the composites. Among the three interface coating combinations investigated, the BN/SiC coated Hi-Nicalon SiC fiber reinforced RBSN matrix composite showed the least amount of uncoated regions and reasonably uniform interface coating thickness. The matrix cracking stress in SiC/RBSN composites was predicted using a fracture mechanics based crack bridging model.

1. Introduction

For the development of hot section components of next generation engines strong, tough, and lightweight materials that can withstand complex thermal cycling under high stresses and corrosive engine environments are required. For the last two decades, silicon carbide fiber reinforced silicon nitride and silicon carbide matrix composites have been investigated for uncooled and cooled turbine components. For the first generation of SiC fiber reinforced reaction bonded silicon nitride matrix composites (SiC/RBSN) large diameter, ~144 μm, SiC fibers prepared from chemical vapor deposition (CVD) were used as a reinforcement (ref. 1). This composite exhibited strong and tough composite behavior, notch insensitive strength, and excellent thermal shock resistance. In addition, this composite served as a model high temperature system to understand structure and property relationships. However this composite cannot be pursued for component development for three reasons. First, there is limited complex shape capability because the large diameter fibers cannot be bent to a radius <1 mm. Second, machining components from a block of composite is very expensive and time consuming. Third, the composite exhibits poor oxidation resistance in the intermediate temperature range from 750 to 1000 °C because of the internal oxidation of the porous RBSN matrix, and oxidation of the carbon at the fiber/matrix interface. Studies have shown that internal oxidation of RBSN can be avoided by infiltrating the RBSN composites with a silicon nitride yielding polymer or by surface coating the RBSN composites with a layer of CVD SiC or Si_3N_4 (refs. 2 and 3). Results indicate that under unstressed conditions the CVD surface coated RBSN composites can survive at 1600°C for 10 hrs in burner rig tests (ref. 4). The first two issues can be resolved by employing smaller diameter (~14 μm) SiC fibers and developing alternate processing approaches for SiC/RBSN composites.

Polymer derived small diameter SiC fibers such as CG Nicalon™ and Tyrranno™ fibers that were coated

with a thin layer (<1 μm) of carbon or BN have been explored earlier as reinforcement for RBSN (refs. 5 to 7). Although in most cases limited strain capability beyond matrix fracture was demonstrated, the ultimate fracture strength was low because of strength degradation of the fibers during high temperature nitridation. In recent years, second-generation small diameter SiC fibers such as Hi-Nicalon^{TM}, Hi-Nicalon-S^{TM}, UBE-SA^{TM}, and Sylramic^{TM} fibers with better thermal stability than the first generation SiC fibers have been developed (refs. 8 and 9). In an earlier study, the microstructural and strength stability of uncoated and CVD coated Hi-Nicalon SiC fibers after heat treatment at temperature to 2000°C in N_2 for up to 400 hr have been investigated (ref. 10). Results of this investigation indicate that this fiber is stable in pure N_2 at least up to 1400°C. Following this investigation, Bhatt and Hull (ref. 11) studied strength properties of pyrolytic boron nitride (PBN), PBN/Si-rich PBN, and boron nitride (BN)/SiC coated Hi-Nicalon SiC fiber/RBSN tow composites processed at 1200 and 1400°C in N_2. This study concluded that all three CVD coated Hi-Nicalon SiC fibers are stable under RBSN processing conditions at 1200°C, but fibers processed at 1400°C have significantly lower strength when compared with the dry bundle strength of the as-received tows. Because of the fiber degradation under processing conditions, the traditional processing methodology and nitridation cycle developed for monolithic RBSN cannot be used for the fabrication of RBSN composites reinforced by small diameter SiC fibers. Therefore Bhatt and Palczer (ref. 12) have developed a low temperature, short time nitridation cycle by controlling the particle size, hence surface area, of the silicon powder.

The objectives of this study were to develop a processing approach for fabricating small diameter SiC fiber reinforced RBSN composites, to evaluate the effects of interface coating on room temperature mechanical properties, and to select the best interface coating for future development of RBSN composites.

2. Experimental procedure

2.1. Materials

The Hi-Nicalon^{TM} SiC fiber spools, required for composite fabrication, were procured from Dow Corning Corporation, Midland, Michigan. A typical fiber tow within the spool contains 500 filaments with filament diameters ranging from 8 to 16 μm. The average diameter of the filament as reported by the company is 14 μm. The as-received fiber tows were coated with one of three interface coatings: a single layer of ~1 μm thick PBN; a dual layer of ~0.5 μm thick PBN followed by ~0.5 μm thick Si-rich PBN; or a dual layer of ~0.8 μm thick BN followed by ~0.2 μm thick SiC. All coatings were applied by CVD. Advanced Ceramics Corporation, Cleveland, Ohio applied the first two coatings and 3M Corporation, Minneapolis, Minnesota applied the last.

Commercial grade silicon powder (Silicomill^{TM} grade-IV supplied by Kemanord, Ljungaverk, Sweden) was used as starting material for slurry preparation for the RBSN matrix. However, the particle size range of the powder was too big to infiltrate between filaments in the tow. Therefore, the as-received silicon powder was wet attrition milled in stoddard solvent (a kerosene-based liquid) for 48 hr to reduce its particle size. A Si_3N_4 grinding medium was used to carry out the milling. The weight ratio of Si powder to grinding media was ≈40. The attrition milling was accomplished by the procedure detailed elsewhere (ref. 13). After grinding, the excess grinding fluid was siphoned off from the vessel, and the silicon slurry was poured into a rectangular pan and dried for 24 hr in a vacuum oven set at 600°C. The dried powder was transferred to a glass jar and stored in a glove box that was purged continuously with high purity nitrogen. In some attrition milling batches, 2.5 wt% NiO was also added to the silicon powder to study the influence of this nitridation enhancing additive on the composite mechanical properties.

The impurities in, and the particle size range and specific surface area of the Si powders were determined respectively, by wet chemistry, laser light scattering (Microtrac, Model 991), and the three point Brunauer-Emmett-Teller (BET) adsorption (Micromeritics, Model ASAP 2010) techniques.

2.2. Composite fabrication

A silicon slurry was prepared by ball milling 30 wt% attrition milled silicon powder, 5 wt% polybutyl methacraylate (PBMA), 4 wt% dibutyl phthalate, 1 wt% fish oil, and 60 wt% isopropyl alcohol. The Hi-Nicalon SiC fiber tow was passed through a series of rollers to spread the tow and then into a tank filled with the silicon slurry. The slurry coated fiber tows were wound on a metal drum at a predetermined spacing to prepare a 150-mm wide fiber mat. After drying in air, the fiber mat was removed from the drum, and cut into 150 × 150-mm pieces. Each piece was then coated with 0.5 mm of silicon slurry by using a doctor blade apparatus. The composition of the slurry was similar to that used for coating the fiber tows. When dried, each piece was cut into 6-mm wide strips; some pieces were cut parallel and others transverse to the fiber tows. Eleven strips, either all-unidirectional or alternate strips of unidirectional and transverse lay-up, were stacked in a stainless steel die and prepressed at 3.5 MPa at room temperature. The prepressed composites were hot pressed at 40 MPa at 800°C for 15 min and then the load was released. Subsequently the temperature was increased to 1200°C and the panel was nitrided for 4 hr in flowing nitrogen. The final dimensions of the specimens after hot pressing were 150 × 12 × 2.5-mm.

The composite panels were surface ground with a diamond particle impregnated metal bonded grinding wheel to remove the excess matrix layer present on the surface. The densities of the composites were calculated by measuring the physical dimensions and the weight, and by also the Archimedes method.

Some of the specimens were sectioned normal to the fibers, mounted in a metallographic mold, ground successively on 40 μm down to 1 μm diamond particle impregnated metal disks, and polished in a vibratory polisher on a micro cloth using 0.3 μm diamond powder

paste. The mounted specimens were coated with a thin layer of carbon or palladium in a vacuum evaporator to avoid charging during observation in a scanning electron microscope (SEM).

The transmission electron microscope specimens were prepared using a procedure similar to that described in reference 14. To describe the procedure briefly, the composite specimens were sectioned into 1-mm slices using a diamond saw, vacuum infiltrated with epoxy and cured at 130°C for 15 min. An ultrasonic drill was used to cut 3-mm diameter disks which were mechanically ground from both sides to 120 μm, dimpled 50 μm from each side, argon ion-beam thinned to perforation, and coated with carbon. A Phillips Model EM400T transmission electron microscope (TEM) operating at 120 KV was used for bright field imaging and convergent beam electron diffraction (CBED). The TEM was equipped with an energy dispersive x-ray spectrometer (EDX) for chemical identification. Some of the TEM specimens were also examined under a Hitachi Model S4700-S field emission scanning electron microscope (FESEM).

For tensile testing, dog-bone shaped specimens were machined from the composite block by using an ultrasonic SiC slurry impact machine. At each specimen end, two glass fiber-reinforced epoxy tabs of dimension 37 × 12 × 1-mm were bonded, leaving ~60-mm for the gauge section. A spring loaded contact extensometer was attached at the center of the gauge section to monitor the strain during the tensile test. The specimens were tested at room temperature until failure in a servo-controlled tensile testing machine equipped with self-aligning grips at a crosshead speed of 1.3 mm/min. The fractured specimens were coated with a thin layer of carbon and then observed by SEM for fracto-graphic analysis.

The fiber push-in tests were performed using a desktop apparatus equipped with capacitance gauges for displacement measurement (ref. 15). The Hi-Nicalon SiC fibers were pushed-in using a 70°-included-angle conical diamond indenter with a 10 μm diameter flat on the bottom. To prevent the sides of the conical indenter from indenting the matrix, the push-in distances were restricted to just a couple of microns. Each test consisted of an initial loading up to a selected maximum load followed by an unloading to zero load and then a reloading to the same maximum load.

3. Results and discussion

The particle size, surface area, and impurity analysis data for the as-received and 48-hr-attrition-milled Si powders are shown in Table I. The as-received Si powder contained Fe and oxygen as major impurities. After 48-hr-attrition-milling, the average particle size decreased and the surface area increased, as expected, but the amount of Y, Al, and oxygen impurities also increased. The amount of Y and Al impurities for the 48-hr-attrition-milled powders reached values of ≈1700 and 200 ppm, respectively. The source of these impurities was traced to the Si_3N_4 grinding media, which contained 6 wt% Y_2O_3 and 2 wt% Al_2O_3 as sintering additives. In batches containing NiO additive, up to 2 wt% Ni was detected in 48-h-attrition-milled powder, in agreement with ~2.5 wt% of intentionally added NiO.

TABLE I Particle size, surface area, and impurity analysis for as received and 48-hr-attrition milled kemanord silicon powder

	As-received	48-Hr-attrition milled
Average particle size (μm)	23.12	0.48
Specific surface area (m^2/g)	1.3	63
Impurities (wt%)		
Carbon	0.01	2.92
Oxygen	0.7	8.87
Iron	0.02	0.02
Impurities (ppm)		
Nickel	6	6[a]
Aluminum	2	200
Chromium	2	2
Yttrium	2	0.17 (wt%)

[a]Batches containing NiO additive showed ~2 wt% Ni.

TABLE II Physical property data for Hi-Nicalon SiC/RBSN composites

Interface coating	Fiber lay-up	Fiber volume (%)	Density (gm/cc)	Porosity (%)
None	0	23 ± 2	1.90	38
PBN	0	22 ± 2	1.98 ± 0.13	36
PBN/Si-PBN	0	21 ± 3	1.92 ± 0.04	38
PBN/Si-PBN	0/90	21 ± 3	1.91 ± 0.05	38
BN/SiC	0	24 ± 1	1.96 ± 0.03	36
BN/SiC	0/90	24 ± 2	1.94 ± 0.01	37

3.1. Physical properties

The room temperature density and porosity of one- and two-dimensional SiC/RBSN composites are shown in Table II. Each data point and corresponding standard deviation in this table represents an average of three test results. The table indicates that the composites contain ~23 vol% fibers and ~37 vol% porosity.

3.2. Microstructure

To determine the degree of matrix infiltration between filaments in the fiber tows and processing defects, cross-sections of one- and two-dimensional reinforced uncoated and three CVD coated Hi-Nicalon SiC/RBSN composites were examined by optical microscopy. A typical cross-section of one-dimensional BN/SiC coated Hi-Nicalon SiC/RBSN composite is shown in Fig. 1. This figure shows that the Si_3N_4 matrix well infiltrated between filaments within the tows, but distinct matrix rich regions exist between the fiber tows. Also notice that the RBSN matrix contains micron sized porosity with some isolated large pores throughout the cross-section. The SEM micrographs of the cross-sections of PBN and BN/SiC coated Hi-Nicalon/RBSN composites show that the CVD interface coatings on Hi-Nicalon fibers are non-uniform and irregular (Fig. 2). These two coatings represent coatings supplied by two different vendors offering two different processing conditions. It is obvious in Fig. 2 that the thickness of the coating on the fibers decreases drastically from the periphery to the center of the tows, and in some

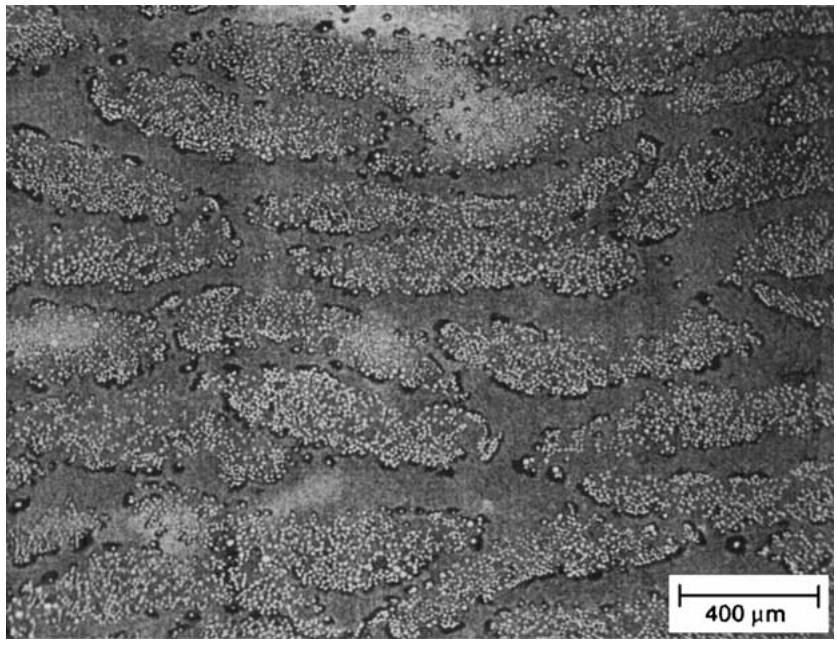

Figure 1 Optical micrograph of the cross-section of a 1-D BN/SiC coated Hi-Nical$_{ODI}$ SiC/RBSN composite ($V_f \sim 0.24$) showing infiltration of silicon nitride matrix between the filaments within the fiber tows, and matrix rich regions between the fiber tows.

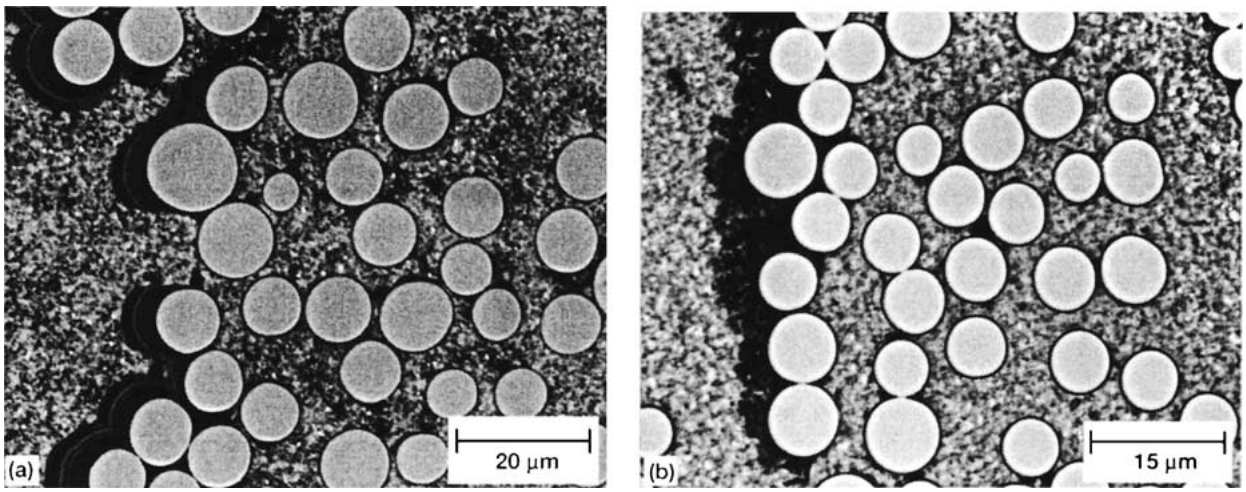

Figure 2 SEM micrographs of the cross-section of the CVD coated Hi-Nicalon SiC/RBSN composites ($V_f \sim 0.24$) showing variation in interface coating thickness from the outer to interior regions of the tow: (a) PBN/Si-rich PBN coated, (b) BN/SiC coated.

cases the fibers at the center of the tows do not even contain the coating (Fig. 2a). However, when the three coatings are compared, the BN/SiC coating appears to be the most uniform. A higher magnification photograph of the cross-section of the composites indicates that the uncoated and nonuniformly coated regions are prevalent where three or more fibers are touching each other (Fig. 3). Quantitative analysis was performed to determine the fraction of uncoated fibers in all three coated composites. Results show that the number of uncoated filaments within the coated tows vary from tow to tow and between the types of the coated fibers. In general, PBN, PBN/Si-PBN, and BN/SiC coated Hi-Nicalon SiC/RBSN composites contained up to 30, 25, and 10 percent uncoated fibers, respectively.

TEM analysis was performed to determine phase stability of the coating and possible reaction between the SiC fiber and RBSN matrix, or between the interface coating and RBSN matrix. In addition, the reaction between NiO and uncoated SiC fibers, and between NiO and the interface coating(s) were also investigated. Results are shown in Figs 4 and 5. A bright field TEM micrograph of the transverse cross-section, and EDX analysis across the fiber/matrix interface of the uncoated Hi-Nicalon SiC/RBSN composites without NiO show no evidence of a solid state reaction between the Hi-Nicalon fiber and RBSN matrix (Figs 4 and 5). On the other hand, the uncoated Hi-Nicalon SiC/RBSN composites containing NiO show chemical reaction wherever the NiO particles are in contact with the fibers (Fig. 6). The average thickness of the reaction zone is $\sim$0.1 μm. EDX analysis indicates that the reaction zone contains Fe and Ni (Fig. 7). Characterization of the SAD pattern indicates that the reaction zone is

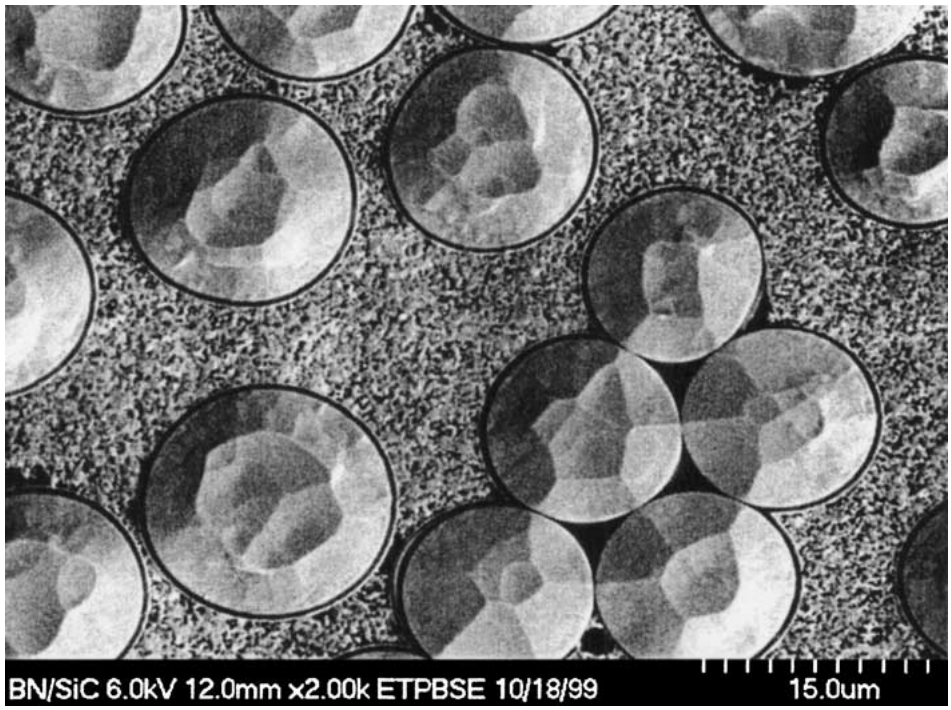

Figure 3 FESEM micrograph of the cross-section of the BN/SiC coated Hi-Nicalon SiC/RBSN composite ($V_f \sim 0.24$) showing uncoated regions in a cluster of fibers.

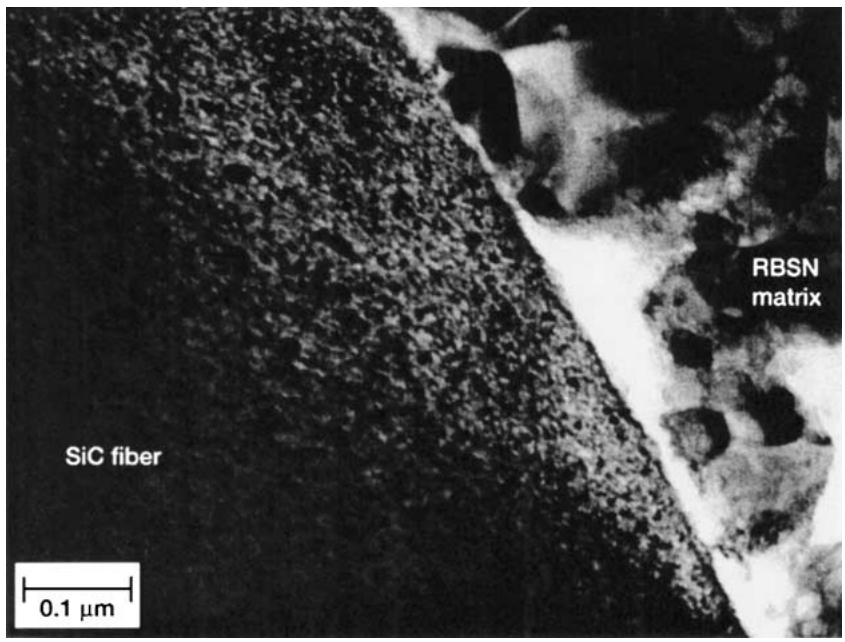

Figure 4 TEM micrograph of the fiber/matrix interface of an uncoated Hi-Nicalon SiC/RBSN composite ($V_f \sim 0.24$) without NiO showing a sharp boundary between the SiC fiber and RBSN matrix.

composed of Fe and Ni silicides (ref. 11). The presence of Fe can be traced to the silicon powder.

TEM examination of the interface zone of the composites indicates that except for the SiC coating all other coatings consist of several layers (Fig. 8). The PBN, Si-PBN and BN coatings are amorphous and the SiC coating is crystalline and nodular. In some specimens, these layers were debonded. It is not clear whether debonding occurred during specimen preparation or pre-existed. No chemical reaction was observed between the Hi-Nicalon SiC fibers and the PBN or the BN coating, or between the outer coating and RBSN matrix. However, wherever NiO came in contact with the fiber coating, or the uncoated region of the fibers, chemical reaction was noticed. These observations are in agreement with the results reported in reference 11.

EDX analysis across the PBN, PBN/SiPBN, and BN/SiC coatings indicates small amounts of Si, O, and C impurities in the BN or PBN coatings (Fig. 9). Whether silicon in the BN coating is an artifact due to smearing during polishing or silicon diffusing into the coating during processing is not known.

Based on TEM and SEM results we conclude that coatings of PBN, PBN/Si-rich PBN, and BN/SiC provided adequate protection of the Hi-Nicalon SiC fibers from reaction with the Fe and Ni, but the CVD coating

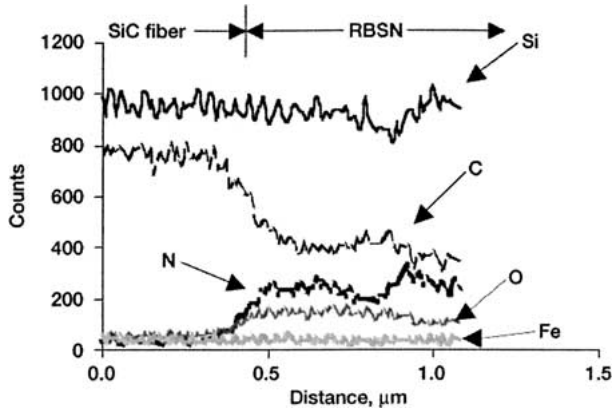

Figure 5 EDX line profile across the fiber/matrix interface region of an uncoated Hi-Nicalon SiC/RBSN composite without NiO additive showing no apparent reaction between the SiC filament and RBSN matrix.

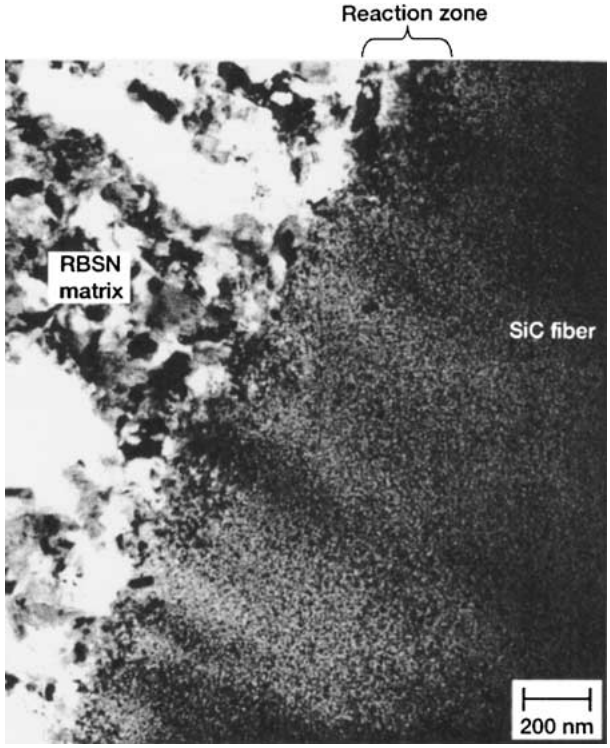

Figure 6 TEM micrograph of the fiber/matrix interface region of an uncoated Hi-Nicalon SiC/RBSN composite ($V_f \sim 0.24$) with NiO showing reaction between the SiC fiber and NiO additive.

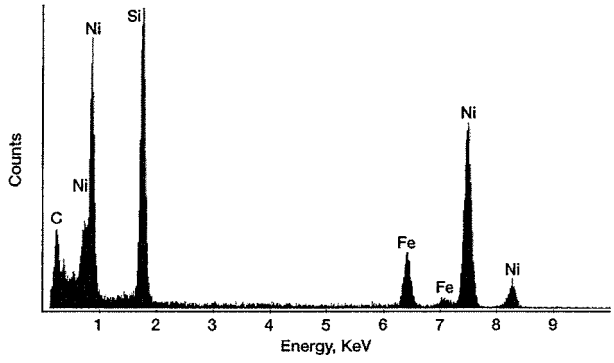

Figure 7 EDX analysis of the reaction zone in Fig. 6 indicates formation of silicides.

process must be optimized to avoid uncoated regions on the fibers.

3.3. Mechanical Behavior

3.3.1. Influence of nitridation enhancing additive, NiO, on mechanical behavior

Transition metals and their oxides are generally used as nitridation enhancing additives in RBSN processing to reduce the processing temperature and time. In monolithic RBSN these additives have no significant influence on the strength. However, in SiC fiber reinforced RBSN composites, these additives react with bare fiber as well as fiber coatings as reported earlier. To determine the influence of this reaction on tensile properties, uncoated and BN/SiC coated Hi-Nicalon SiC fiber reinforced RBSN composites with and without NiO additives were tensile tested at room temperature. The results are shown in Figs 10 and 11. In these figures, the stress-strain curves are displaced by 0.05 percent strain for better clarity. These figures indicate that the ultimate strength values of uncoated and BN/SiC coated Hi-Nicalon SiC/RBSN composites containing NiO additives are slightly lower than those of the composite fabricated without NiO. However, these strength values are well within the scatter band of strength measured for these composites. Therefore, it appears that the nitridation-enhancing additive, NiO, hence NiO/SiC reaction, may not have a significant effect on tensile properties of the composite.

3.3.2. Influence of interface coating on mechanical behavior

Room temperature tensile stress-strain behaviors of unidirectional reinforced uncoated, PBN, PBN/Si-PBN, and BN/SiC coated (∼24 vol%) Hi-Nicalon SiC/RBSN composites containing NiO additive are shown in Fig. 12. In Fig. 12, the strain scale of PBN and PBN/Si-PBN coated, and uncoated Hi-Nicalon SiC/RBSN composites is deliberately displaced by 0.05, 0.1, and 0.15 percent respectively, to distinguish the stress-strain behaviors. The stress-strain curves of the uncoated Hi-Nicalon SiC/RBSN composites exhibited a linear elastic behavior until fracture. This suggests that the matrix cracks do not deflect at the fiber matrix interface either because of a strong bond formed between the fiber and the matrix under the processing conditions of the composites or because of the large tensile residual stress acting upon the fiber. On the other hand, the stress-strain curve of the PBN, PBN/Si-PBN, and BN/SiC coated Hi-Nicalon/RBSN composite shows an initial elastic region followed by a nonlinear region. The nonlinear region for the PBN and PBN/Si-PBN coated Hi-Nicalon SiC/RBSN composites is much shorter than that for the BN/SiC coated Hi-Nicalon/RBSN composite.

Typical room temperature tensile stress-strain behavior of $[0]_{10}$ and $[0_5/90_5]_S$ BN/SiC coated Hi-Nicalon SiC/RBSN composites (∼24 vol%) is shown in Fig. 13. The stress-strain curves of the one- and

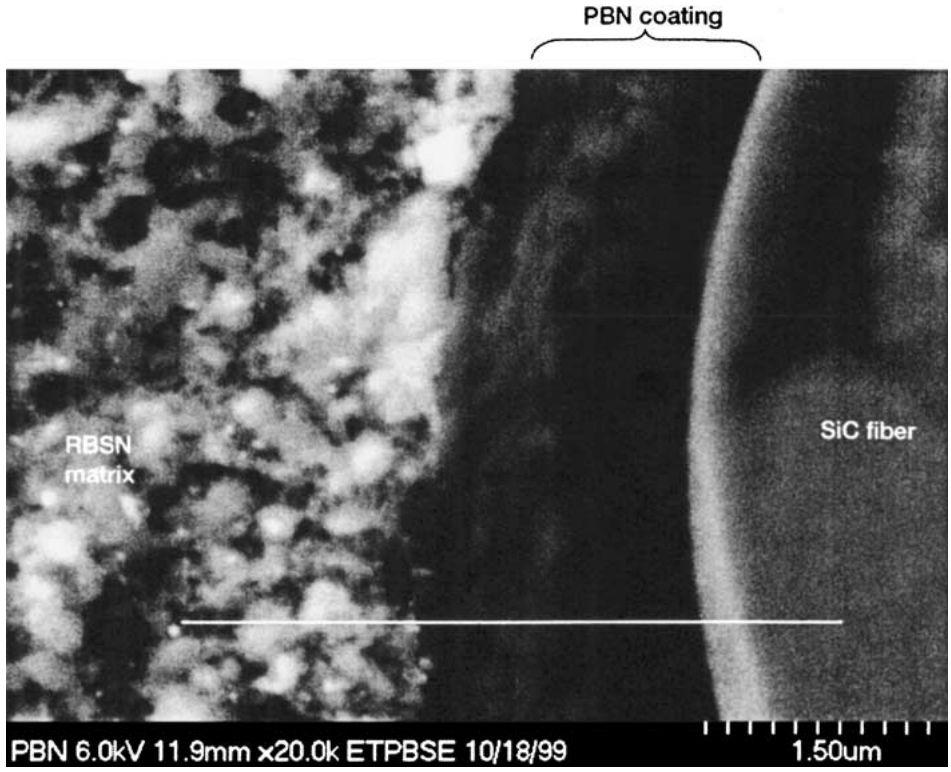

Figure 8 FESEM micrograph of the interface region of a PBN coated Hi-Nicalon SiC/RBSN composites with NiO additive.

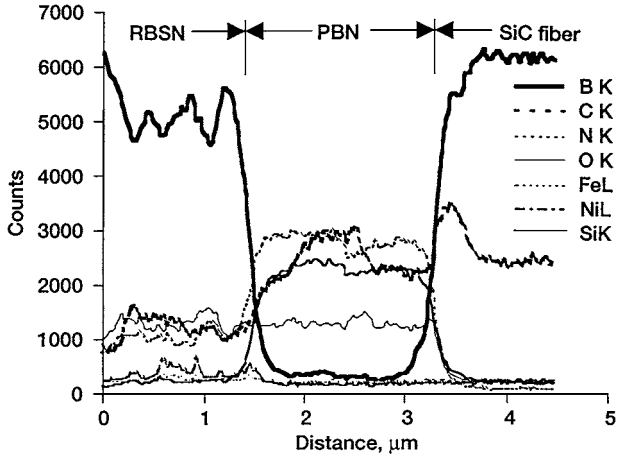

Figure 9 EDX line profile across the indicated region in Fig. 8.

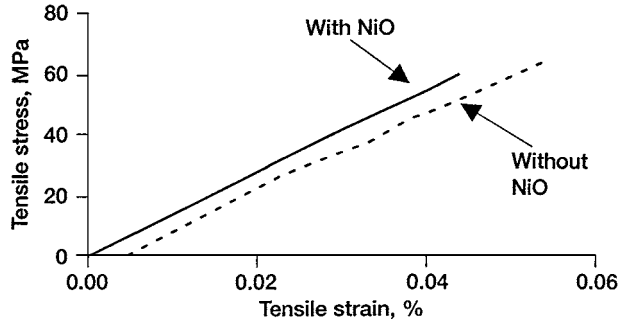

Figure 10 Room temperature tensile stress–strain behavior for 1-D uncoated Hi-Nicalon SiC/RBSN composites ($V_f \sim 0.24$) with and without NiO additive.

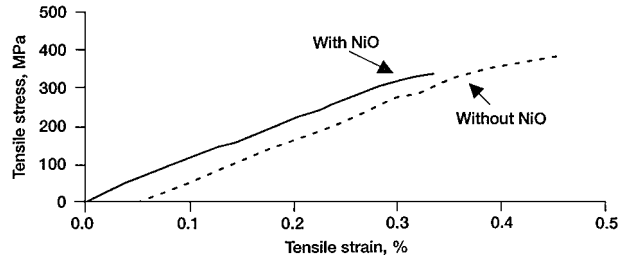

Figure 11 Room temperature tensile stress–strain behavior for 1-D BN/SiC coated Hi-Nicalon SiC/RBSN composites ($V_f \sim 0.24$) with and without NiO additive.

two-dimensional reinforced BN/SiC coated Hi-Nicalon SiC/RBSN composites show two distinct regions: an initial linear region followed by a non-linear region. At ultimate load the composite specimens failed abruptly. The tensile data for the one- and two-dimensional RBSN composites reinforced by uncoated and three CVD coated Hi-Nicalon SiC fibers are tabulated in Table III.

Fig. 14 shows the fracture surfaces of one- and two-dimensional BN/SiC coated Hi-Nicalon SiC/RBSN composites. In some regions of the fracture surface, flat fracture is noticed, while other regions exhibited significant amount of fiber pullout, typical of a tough composite. In the flat fracture regions, the fibers appear to have no interface coating. When the fractured specimen was viewed edge on, no multiple matrix cracks were observed. This suggests that the matrix cracks are closed upon unloading the fractured specimen or that the fracture process is localized near the fracture surface.

3.4. Interfacial shear strength

The fiber push-in tests were performed at room temperature to measure interfacial shear strength properties of each composite. The data were analyzed by subtracting

the appropriate load-train compliance correction from the measured displacements. The fiber debond initiation stress was determined and the frictional sliding stresses were estimated. An estimate of frictional sliding stress, τ, was made using the constant τ model of Marshall and Oliver (ref. 16) by fitting the following relationship to the reloading curves:

$$u = u_o + F^2/8\pi^2 r^3 E_f \tau$$

where u is the fiber end displacement, u_o is the residual fiber end displacement after the previous unloading, F is the applied load, r is the fiber radius, and E_f is the fiber modulus. In addition, a debond initiation stress, σ_d, could be calculated from the debond initiation load, F_d, (the load at which fiber end begins to move) by the relation, $\sigma_d = F_d/\pi r^2$.

3.4.1. Influence of nitride enhancing additive, NiO, on interfacial shear

Many of the push-in tests of uncoated fibers could not be successfully completed due to the very high fiber/matrix bonding for uncoated fibers. For this reason, meaningful averages of debond initiation and frictional sliding stresses could not be obtained. However, a significant effect of the presence of the NiO additive was still evident from comparing the fraction of fibers that could be successfully debonded and pushed in for the uncoated SiC/RBSN composites with and without the NiO additive (Fig. 15). In the case of uncoated SiC/RBSN composites containing no NiO, a large fraction of the fibers can be debonded, but these fibers are difficult to slide. On the other hand, in the uncoated SiC/RBSN composites containing NiO, a large fraction of the fibers could not be debonded at all; significant fiber damage occurred before debonding could be achieved. These differences in interfacial behavior can be analyzed based on surface roughness of the fibers, and the chemical reaction between the fiber and the NiO additive. Although there is no evidence of chemical reaction between uncoated SiC fiber and RBSN matrix without NiO (Figs 4 and 5), roughening of the fiber surface can occur because of the Si_3N_4 grains indenting on the fibers during fabrication. As a result even though it is easier to debond the fiber, pushing the roughened fibers out of the RBSN matrix during push-in test is difficult without damaging the fibers. In contrast, in the uncoated SiC/RBSN composites containing NiO, chemical reaction is seen in regions where the NiO additive in matrix encountered the fiber (Figs 6 and 7). The strong bond formed between the SiC fiber and matrix results in high interfacial debond strength.

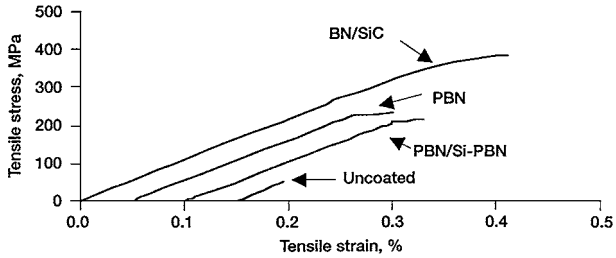

Figure 12 Typical room temperature tensile stress–strain behavior for 1-D uncoated, PBN, PBN/Si-rich PBN, and BN/SiC coated Hi-Nicalon SiC/RBSN composite ($V_f \sim 0.24$) with NiO additive.

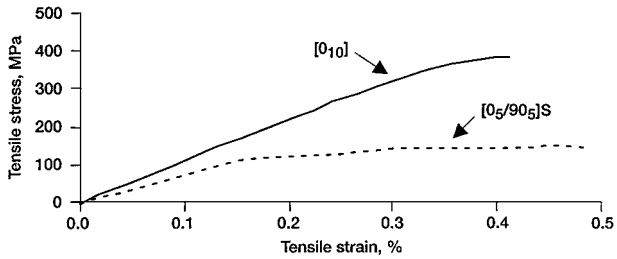

Figure 13 Comparison of room-temperature tensile stress curves of 1-D and 2-D BN/SiC coated Hi-Nicalon SiC/RBSN composites ($V_f \sim 0.24$) with NiO additive.

3.4.2. Influence of interface coating on interfacial shear

The load-displacement curves generated from the push-in tests for the three-coated Hi-Nicalon SiC/RBSN composites containing NiO additive are similar. A typical load-displacement curve for the one-dimensional BN/SiC coated Hi-Nicalon SiC/RBSN composites with NiO additive is shown in Fig. 16. According to this figure, initially the displacement increases with increase in load up to a critical load level at which the fiber debonded from the matrix. Beyond this point the load momentarily decreased and then again increased with increasing displacement. The interfacial property data for the composites with coated and uncoated fibers are summarized in Table IV. Each data point and the corresponding standard deviation in the table represent an average of 8 to 21 tests on coated fibers; meaningful averages for the composite with uncoated fibers could not be obtained because the fiber/matrix bond was too strong for most of the tests to achieve fiber/matrix debonding. As stated earlier, 10 to 30 vol% of the fibers

TABLE III Mechanical property data for Hi-Nicalon SiC/RBSN composites with NiO additive

Interface coating	Fiber lay-up	Fiber volume (%)	Proportional limit stress (MPa)	Proportional limit strain (%)	Elastic modulus (GPa)	Ultimate tensile strength (MPa)	Ultimate tensile strain (%)
None	0	23 ± 2	36 ± 11	0.03 ± 0.01	133 ± 13	52 ± 13	0.10 ± 0.01
None	0/90	23 ± 2	31	0.04	90	31	0.04
PBN	0	22 ± 2	102 ± 48	0.1 ± 0.04	96 ± 15	195 ± 46	0.20 ± 0.01
PBN/Si-PBN	0	21 ± 3	80 ± 1	0.1 ± 0.01	96 ± 38	152 ± 31	0.14 ± 0.04
PBN/Si-PBN	0/90	21 ± 3	65 ± 4	0.1 ± 0.01	68 ± 7	82 ± 8	0.13 ± 0.01
BN/SiC	0	24 ± 1	290 ± 21	0.28 ± 0.02	105 ± 1	329 ± 8	0.27 ± 0.13
BN/SiC	0/90	24 ± 2	88 ± 18	0.12 ± 0.03	73 ± 3	133 ± 22	0.35 ± 0.09

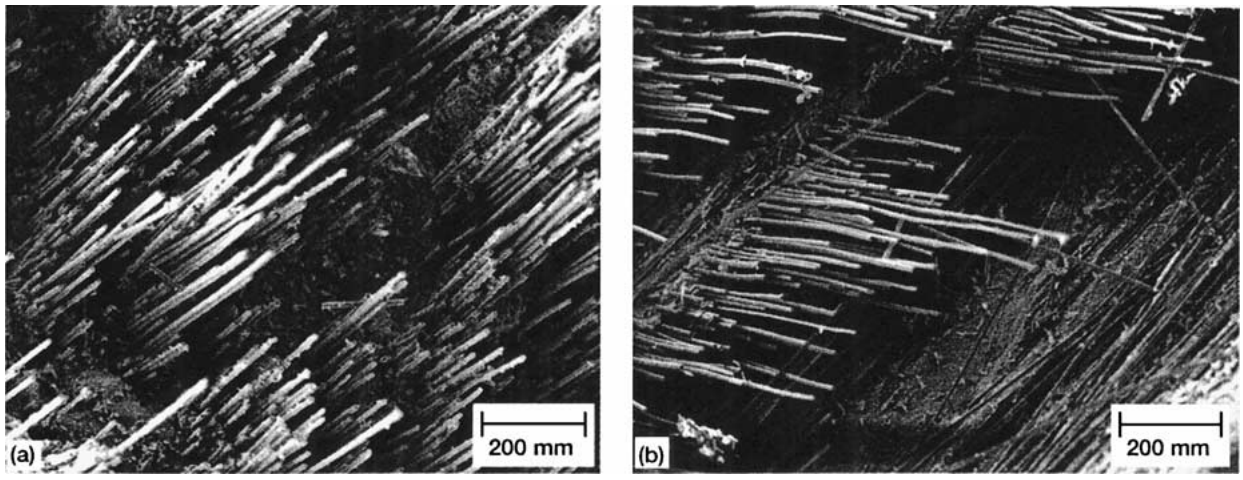

Figure 14 SEM photographs of the tensile fracture surfaces of BN/SiC coated Hi-Nicalon SiC/RBSN composites ($V_f \sim 0.24$): (a) 1-D, (b) 2-D.

TABLE IV Influence of coating composition on interfacial properties for Hi-Nicalon SiC/RBSN composites with NiO additive

Interface coating	Debond stress (GPa)	Frictional stress (MPa)
None	>5	~340
PBN	0.54 ± 0.33	14.4 ± 6.26
PBN/Si-PBN	0.26 ± 0.07	4.55 ± 3.45
BN/SiC	0.51 ± 0.45	12.6 ± 10.9

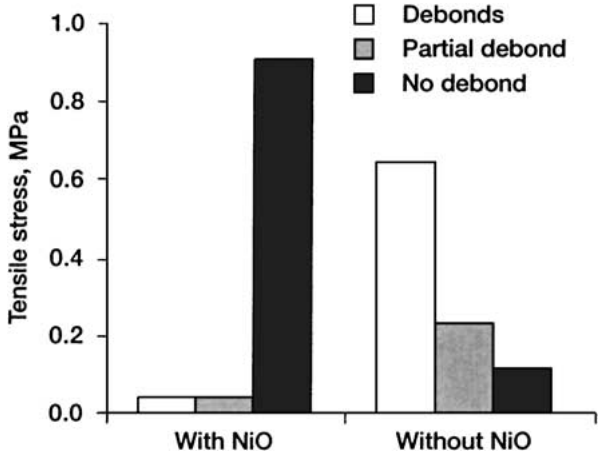

Figure 15 Influence of nitridation enhancing additive, NiO, on interfacial debonding properties of uncoated Hi-Nicalon SiC/RBSN composites ($V_f \sim 0.24$).

were found to contain uncoated regions in the coated composites. The interfacial frictional shear strength of the poorly coated fibers reached values similar to those of uncoated composites (Fig. 17). This shows that in order to obtain reproducible interfacial shear properties, poorly coated and uncoated regions must be avoided.

3.5. Matrix cracking strength prediction

A fiber bridging crack model developed by Aveston, Cooper, and Kelly (ref. 17) was used to predict the matrix cracking strength. The following expression for predicting the steady state matrix cracking strength (σ_{ss}) was used.

$$\sigma_{ss} = \left[6\tau_f \Gamma_m V_f^2 E_f E_C^2 / R V_m E_m^2\right]^{1/3} \quad (1)$$

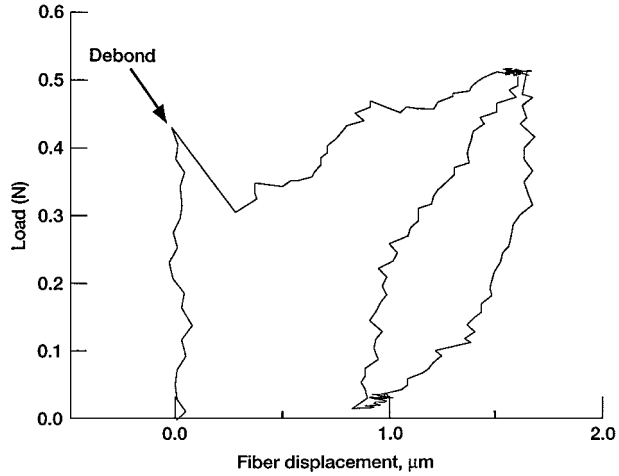

Figure 16 Typical fiber push-in test behavior for the BN/SiC coated Hi-Nicalon SiC/RBSN composites.

where E_f, E_m, and E_C are the elastic moduli of the fiber, the matrix, and the composite (in the longitudinal direction), respectively, τ_f is the interfacial frictional shear strength, R is the fiber radius, Γ_m is the matrix fracture energy, V_f is the fiber volume fraction, and V_m is the matrix volume fraction. Accounting for the (longitudinal) thermal residual stresses due to mismatch in the thermoelastic properties between the fiber and matrix in equation (1).

$$\sigma_{cr} = \sigma_{ss} + \sigma_R \quad (2)$$

and σ_R can be approximated by

$$\sigma_R = (\alpha_f - \alpha_m)\Delta T\, E_f V_f \quad (3)$$

where α_f and α_m are the linear thermal expansion coefficients of the fiber and the matrix, respectively, and ΔT is the temperature differential during processing. The variation of matrix cracking strength with fiber fraction was predicted with and without accounting for thermal residual stresses using the values: $E_f = 270$ GPa, $E_m = 60$ GPa, $\Gamma_m = 36$ J/m^2, $\alpha_f = 3.8 \times 10^{-6\circ}$/C, $\alpha_m = 5.4 \times 10^{-6}/^\circ$C, $\tau = 15$ MPa, $\Delta T = 1175^\circ$C and $R = 7$ μm. Predicted results and the measured values are plotted in Fig. 18. The plot indicates that the

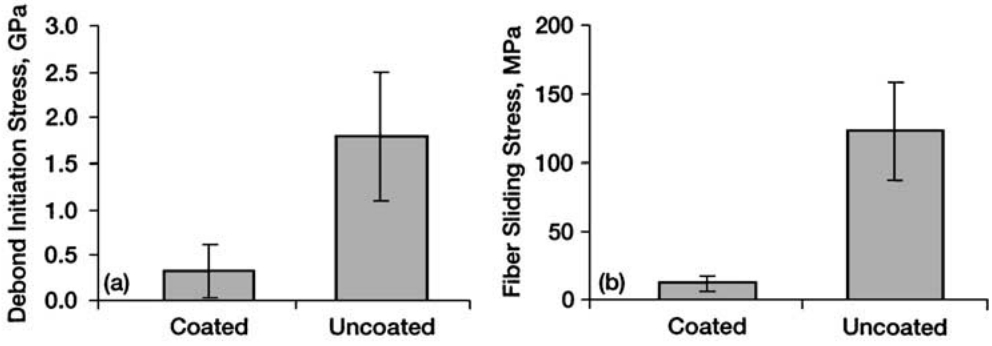

Figure 17 Influence of interface coating on interfacial properties of PBN coated Hi-Nicalon SiC/RBSN composites ($V_f \sim 0.24$) with NiO: (a) fiber debond stress, (b) fiber sliding stress.

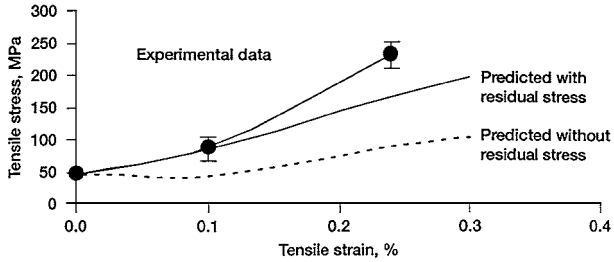

Figure 18 Experimental data and predictions of first matrix cracking stress using the long fiber-bridging crack model for the BN/SiC coated SiC/RBSN composites.

predicted values for the matrix cracking strength accounting for thermal residual stresses agree well with the measured values at low fiber fractions.

4. Summary of results

A processing method for small diameter SiC fiber reinforced RBSN composites has been developed, and the effect of interfacial coating composition and nitridation enhancing additive on the properties of the composites have been determined. Key findings are the following.

(1) Strong and tough small diameter Hi-Nicalon SiC fiber reinforced RBSN composites can be fabricated using fiber lay-up method and a low temperature nitridation cycle.

(2) Significant variation in interface coating thickness and uncoated regions were noticed in PBN, PBN/ Si-PBN, and BN/SiC coated SiC/RBSN composites across the fiber tows.

(3) In the uncoated regions, the fiber surface is roughened and NiO additive reacted with the fibers to form $NiSi_2$ and $FeSi_2$. Both these factors caused degradation of tensile strength in the SiC/RBSN composites.

(4) All three-interface coatings namely the PBN, Si-PBN and BN/SiC are compatible with RBSN matrix. No reaction was observed between these coatings and Hi-Nicalon SiC fibers or RBSN matrix.

(5) The first matrix cracking strength in SiC/RBSN composites can be conservatively predicted using a fiber bridging crack model when residual stresses are taken into account.

5. Conclusions

Strong and tough SiC/RBSN composites can be fabricated using coated SiC tows. However, interface-coating uniformity is a major issue affecting properties of the composites. Further improvements in composite properties are possible by optimizing both the CVD coating process to achieve uniform interface coating thickness, and the fiber lay up process to reduce matrix rich regions.

References

1. R. T. BHATT, NASA TM-88814 (1986).
2. O. J. GREGORY and M. H. RICHMAN, *J. Amer. Ceram. Soc.* **67**(5) (1984) 335.
3. J. DESMAISON, N. ROELS and P. BELAIR, *Mater. Sci. and Engin.* **A121** (1989) 441.
4. W. R. FOHEY, R. T. BHATT and G. Y. BAAKLINI, NASA-CP-19117 (1993) p. 68.
5. J. W. LUCEK, G. A. ROSSETTI, JR. and S. D. HARTLINE, in "Metal Matrix, Carbon, and Ceramic matrix Composites," NASA CP-2406, edited by J. D. Buckley (NASA, Washington, DC, 1985).
6. T. L. STARR, D. L. MOHR, W. J. LACKEY and J. A. HANIGOFSKY, *Ceram. Eng. Sci. Proc.* **14**(9/10) (1993) 1125.
7. G. H. WOBLEWSKA and G. ZIEGLER, in "High-Temperature Ceramic-Matrix Composites II: Manufacturing and Materials Development," edited by A. G. Evans and R. Naslain, *Ceramic Trans.* **58** (1995) 131.
8. M. TAKEDA, Y. IMAI, H. ICHIKAWA, T. ISHIKAWA, N. KASAI, T. SEGUCHI and K. OKAMURA, *Ceram. Eng. Sci. Proc.* **13**(7/8) (1992) 209.
9. J. B. HURST, D. GORICAN and H. M. YUN, in "Advances in Ceramic Matrix Composites III," edited by N. P. Bansal and J. P. Singh, *Ceramic Trans.* **58** (1995) 131.
10. R. T. BHATT and A. GARG, in "Proc. ICCM 10, Eds. A. Poursartip and K. L. Street (1995) Vol. VI, p. 339.
11. R. T. BHATT and D. R. HULL, NASA TM-113170.
12. R. T. BHATT and A. R. PALCZER, *J. Mater. Sci.* **34** (1999) 1483.
13. T. P. HERBELL, T. K. GLASGOW and N. W. ORTH, *Bull. Amer. Ceram. Soc.* **63**(9) (1984) 1176.
14. R. KOCH and A. F. MARSHALL, *Mater. Res. Soc. Symp. Proc.* **199** (1990) 145.
15. J. I. ELDRIDGE, NASA TM-105341 (1991).
16. D. B. MARSHALL and W. C. OLIVER, *Mater. Sci. Eng. A* **126** (1990) 95.
17. J. AVESTON, G. COOPER and A. KELLY, Single and Multiple Fracture, in The Properties of Fiber Composites (Conference Proceedings, National Physical Laboratory, Guildford) (IPC Science and Technology Press Ltd., 1971).

Received 26 October 2000
and accepted 3 August 2001